Patterns of Proteolytic Cleavage and Carbodiimide Derivatization in Sarcoplasmic Reticulum Adenosinetriphosphatase†

Jorge García de Ancos‡ and Giuseppe Inesi*

Department of Biological Chemistry, University of Maryland at Baltimore School of Medicine, 660 West Redwood Street, Baltimore, Maryland 21201

Received July 6, 1987; Revised Manuscript Received September 28, 1987

ABSTRACT: Two series of experiments were carried out to characterize (a) peptide fragments of sarcoplasmic reticulum (SR) ATPase, based on proteolysis with different enzymes and distribution of known labels, and (b) specific labeling and functional inactivation patterns, following ATPase derivatization with dicyclohexylcarbodiimide (DCCD) under various conditions. Digestion with trypsin or chymotrypsin results in the initial cleavage of the SR ATPase in two fragments of similar size and then into smaller fragments, while subtilisin and thermolysin immediately yield smaller fragments. Peptide fragments were assigned to segments of the protein primary structure and to functionally relevant domains, such as those containing the ^{32}P at the active site and the fluorescein isothiocyanate at the nucleotide site. ATPase derivatization with [^{14}C]DCCD under mild conditions produced selective inhibition of ATPase hydrolytic catalysis ($EP + H_2O \rightleftharpoons E + P_i$) without significant incorporation of the ^{14}C radioactive label. This effect is attributed to blockage of catalytically active residues by reaction of the initial DCCD adduct with endogenous or exogenous nucleophiles. ATPase derivatization with [^{14}C]DCCD under more drastic conditions produced inhibition of calcium binding, ^{14}C radioactive labeling of tryptic fragments A_1 and A_2 (but not of B), and extensive cross-linking. Intermolecular and, to some extent, intramolecular cross-linking were prevented by exogenous nucleophiles. The presence of calcium during derivatization prevented functional inactivation, radioactive labeling of fragment A_2, and internal cross-linking of fragment A_1. It is proposed that both A_1 and A_2 fragments participate in formation of the calcium binding domain and that the labeled residues of fragment A_2 are directly involved in calcium complexation. A diagram is constructed, representing the relative positions of labels and functional domains within the ATPase protein.

The calcium pump of sarcoplasmic reticulum (SR)[1] can be studied conveniently in isolated SR vesicles (Hasselbach & Makinose, 1961, 1963; Ebashi & Lipman, 1962) and serves as a model for cation transport coupled to ATP hydrolysis (Hasselbach & Makinose, 1961, 1963; Ebashi & Lipman, 1962; Inesi, 1985). The pump is a Ca^{2+}-dependent ATPase whose primary sequence is now known in its entirety (MacLennan et al., 1985; Brandl et al., 1986). Clarification of the coupling mechanism between ATP utilization and calcium transport would be furthered by identification of protein domains and residues that are actively involved in the partial reactions of the transport and catalytic cycle, such as calcium binding, phosphoryl transfer from ATP to the enzyme, and hydrolytic cleavage of the resulting phosphoenzyme intermediate (E–P). In this regard, considerable progress has been made by the assignment of phosphate (E–P), fluorescein isothiocyanate (FITC) (nucleotide site), iodoacetamide analogues, *N*-ethylmaleimide (NEM), and [(trifluoromethyl)-iodophenyl]diazirine (TID) labels to large fragments obtained by cleavage of the ATPase with trypsin (Thorley-Lawson & Green, 1973; Saito et al., 1984; Andersen et al., 1986; Baba et al., 1986; Squier et al., 1987) and to specific residues in the primary sequence (Allen & Green, 1976; Mitchinson et al., 1982; Saito-Nakatsuka et al., 1987; Yamashita & Kawakita, 1987).

In this study, we describe a series of experiments in which we have characterized the patterns of proteolysis of the ATPase by trypsin, chymotrypsin, thermolysin, and subtilisin and compared the respective distribution of the phosphorylation site and FITC labels. In addition, we have studied the effect of ATPase derivatization with dicyclohexylcarbodiimide (DCCD). Our interest in carbodiimides is related to their role as inhibitors (Pick & Racker, 1979; Murphy, 1981) as well as radioactive (Pick & Racker, 1979) and fluorescent (Scott, 1986; Chadwick & Thomas, 1983) labels.

Interpretation of experiments on derivatization with DCCD is rendered difficult (1) by the different types of inhibition (calcium binding vs hydrolytic catalysis) obtained under various conditions of derivatization (Scofano et al., 1985), (2) the probability that inhibition is related to internal protein cross-linking with elimination of the label (Pedemonte & Kaplan, 1986), and (3) the possibility that some labeled residues are not directly involved in the inhibitory effect. Furthermore, partitioning of the label in the membrane bilayer, as opposed to covalent interaction with protein residues, contributes a large signal in this type of experiment (Scofano et al., 1985). Therefore, we have carried out a detailed characterization of the functional effects, the patterns of

† This work was supported by NIH Grant 5-PO1 HL 27867.

‡ Present address: Unidad de Biomembranas, Instituto de Inmunología CSIC, Velázquez 144, 28006 Madrid, Spain.

[1] Abbreviations: DCCD, dicyclohexylcarbodiimide; DCU, dicyclohexylurea; EDA, ethylenediamine; EDTA, ethylenediaminetetraacetic acid; EGTA, ethylene glycol bis(β-aminoethyl ether)-*N*,*N*,*N*′,*N*′-tetraacetic acid; EP, phosphoenzyme intermediate; FITC, fluorescein isothiocyanate; GEE, glycine ethyl ester; LDS, lithium dodecyl sulfate; MOPS, 3-(*N*-morpholino)propanesulfonic acid; SDS, sodium dodecyl sulfate; SR, sarcoplasmic reticulum; NEM, *N*-ethylmaleimide; MES, 2-(*N*-morpholino)ethanesulfonic acid; Tris, tris(hydroxymethyl)aminomethane; IAEDANS, *N*-(iodoacetyl)-*N*′-(5-sulfo-1-naphthyl)ethylenediamine.

0006-2960/88/0427-1793$01.50/0

proteolytic digestion, and the distribution of radioactive label, following ATPase derivatization with DCCD at low or high concentrations, in the presence and in the absence of calcium, and in the presence and in the absence of exogenous nucleophiles to avoid cross-linking. We have also carried out comparative experiments with other known labels as an aid for the identification of peptides.

Materials and Methods

Reagents. [γ-^{32}P]ATP, [^{32}P]P_i, and $^{45}CaCl_2$ were purchased from New England Nuclear, and [^{14}C]DCCD was from Amersham. DCCD, FITC, proteases, inhibitors, and the molecular weight standards for electrophoresis were obtained from Sigma Chemical Co.

SR Vesicles. These were prepared from white rabbit hind leg muscle as previously described by Eletr and Inesi (1972). Protein concentration was determined by the method of Lowry et al. (1951) using bovine serum albumin as a standard.

Digestion of SR Vesicles. Digestion of SR vesicles (2–5 mg/mL) was carried out in the presence of 20 mM MOPS (pH 6.8) and 80 mM KCl with the following: (a) trypsin at a trypsin/SR ratio of 0.005 for 1–30 min; (b) chymotrypsin at a chymotrypsin/SR ratio of 0.2 or 0.4 for 60 min, treated prior to digestion with trypsin inhibitor at a trypsin inhibitor/chymotrypsin ratio of 0.015; (c) subtilisin at subtilisin/SR ratios from 0.1 to 0.0007 for 30 min; and (d) thermolysin at a thermolysin/SR ratio of 0.5 for 1–90 min, in the presence of 1 mM Ca^{2+}. Tryptic digestion was stopped by adding soybean trypsin inhibitor at a trypsin inhibitor/trypsin ratio of 2, digestion with subtilisin or chymotrypsin was inhibited by adding phenylmethanesulfonyl fluoride to a final concentration of 5 mM, and thermolytic digestion was interrupted by adding EDTA to a final concentration of 5 mM.

Phosphorylation of Digested SR Vesicles. Digested SR vesicles were centrifuged at 40000*g*, the supernatants discarded, and the sediments resuspended in 20 mM MOPS (pH 6.8), 80 mM KCl, 10 mM $MgCl_2$, 0.1 mM $CaCl_2$, and 0.03 mM A23187 to a final protein concentration of 3 mg/mL. The reaction was carried out at 0–4 °C, started with 50 μM [γ-^{32}P]ATP, and quenched after 3 s with 5% trichloroacetic acid and 0.2 mM P_i (final concentration). The samples were then dissolved in denaturing buffer for electrophoresis at pH 6.3.

Fluorescein Isothiocyanate Labeling. SR vesicles were labeled with FITC according to Anderson et al. (1982) with some modifications. SR vesicles (2 mg/mL) were incubated for 20 min (at 25 °C in the dark) in 10 mM Tris, pH 9.2, 80 mM KCl, 0.1 mM EGTA, 20% glycerol, and 40 μM FITC (isomer I). The reaction was stopped by removing the excess of FITC by filtration on Sephadex G-50 columns, using 20 mM MOPS and 80 mM KCl (pH 6.8) as an elution buffer. The elution fractions containing protein were recovered and centrifuged. The protein pellets were resuspended in the appropriate media for proteolytic digestion. In order to measure the stochiometry of bound FITC, the pellets were dissolved in 10 mM Tris, pH 9.2, and 1% SDS; the FITC concentration was estimated by assuming a molar extinction coefficient of 80 000 M^{-1} cm^{-1} at 496 nm (Mitchinson et al., 1982). The protein concentration in these samples was determined by the absorption at 280 nm.

Dicyclohexylcarbodiimide Labeling. SR vesicles (1 mg/mL) were incubated with 200 μM [^{14}C]DCCD (10 mM stock prepared fresh every day) for 2 h at 0–4 °C in 50 mM MES, pH 6.0, 100 mM KCl, 40 μM A23187, and either 50 μM Ca^{2+} or 1 mM EGTA. The reaction was stopped by dilution with 100 mM MOPS (pH 7.0) and by spinning down the vesicles. The pellets were resuspended in appropriate media for proteolytic digestion.

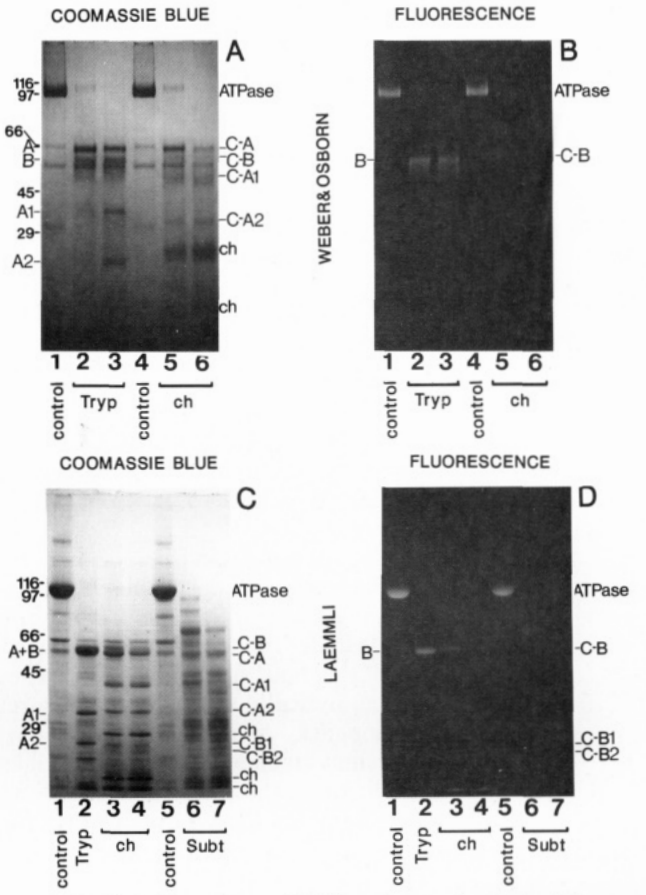

FIGURE 1: Labeling pattern of ATPase fragments obtained by proteolytic digestion of SR vesicles preincubated with FITC. Panels A and B (Coomassie blue and FITC fluorescence, respectively) show electrophoretic patterns (Weber & Osborn, 1969) of nondigested SR vesicles (columns 1 and 4) and of SR vesicles digested with trypsin (0.005 trypsin/SR ratio) for 5 or 30 min (columns 2 and 3) and with chymotrypsin (0.2 or 0.4 chymotrypsin/SR ratio; columns 5 and 6) for 60 min. Panels C and D (Coomassie blue and FITC fluorescence, respectively) show electrophoretic patterns (Laemmli, 1970) of nondigested SR vesicles (columns 1 and 5) and of SR vesicles digested with trypsin (0.005 trypsin/SR ratio) for 30 min (column 2), with chymotrypsin (0.2 or 0.4 chymotrypsin/SR ratio; columns 3 and 4) for 60 min, and with subtilisin (0.001 or 0.002 subtilisin/SR ratio; columns 6 and 7). A, B, A_1, and A_2 and CA, CB, CA_1, CA_2, CB_1, and CB_2 correspond to ATPase tryptic and chymotryptic fragments, respectively; ch indicates the chymotrypsin subunits visible in the gel. Previous to digestion, the SR vesicles were labeled with FITC as described under Materials and Methods.

In order to perform functional studies with the ATPase derivatized with DCCD, labeling of SR vesicles (1 mg/mL) was carried out with either 200 μM DCCD (high DCCD/SR ratio) or 10 μM DCCD (low DCCD/SR ratio) for 2 h at 0–4 °C in the presence of 50 mM MES (pH 6.0), 100 mM KCl, 20% (v/v) glycerol, and 50 μM $CaCl_2$ or 1 mM EGTA and in the presence of either 0.2 M glycine ethyl ester or 0.1 M ethylenediamine when indicated. The reaction was stopped by spinning down the vesicles, and the pellets were resuspended in 10 mM MOPS (pH 7.0) and 30% sucrose. We eliminated the ionophore (40 μM A23187) from our reaction medium, since it inhibited our controls, and we added glycerol to avoid pressure inactivation of the ATPase during the centrifugation to stop the reaction (Champeil et al., 1981; Varga et al., 1986). In order to rule out a direct EGTA effect, in some experiments we did not add EGTA but rather removed Ca^{2+} from our

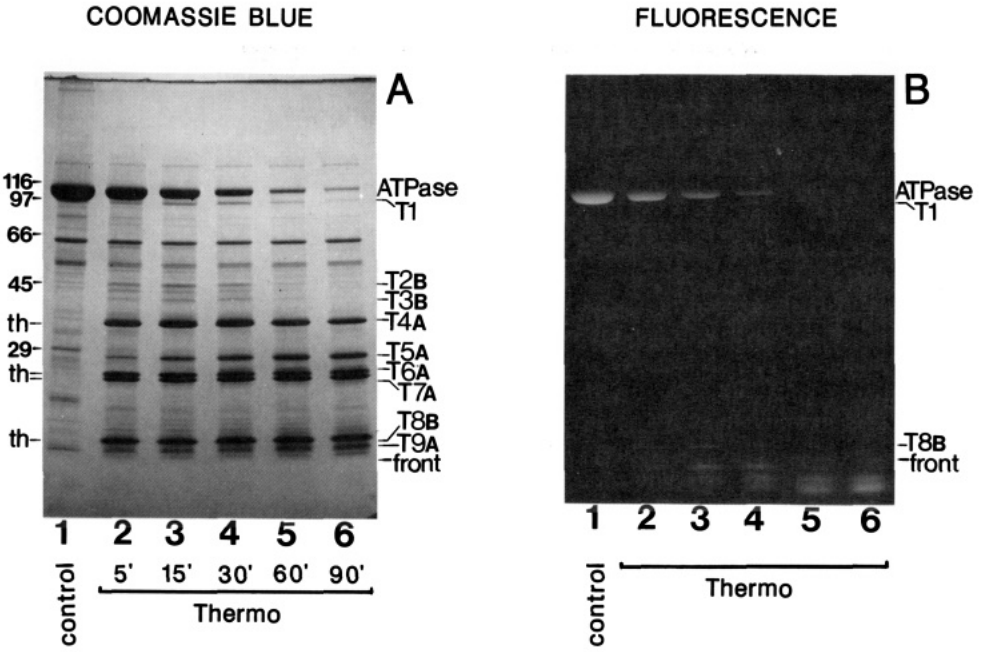

FIGURE 2: Labeling pattern of SR ATPase fragments obtained by digestion with thermolysin of SR vesicles preincubated with FITC. Panels A and B (Coomassie blue and FITC fluorescence, respectively) show electrophoretic patterns (Laemmli, 1970) of nondigested SR vesicles (column 1) and of SR vesicles digested with thermolysin (0.5 thermolysin/SR ratio) for 5, 15, 30, 60, or 90 min (columns 2, 3, 4, 5, and 6, respectively). T_1–T_9 correspond to SR ATPase thermolytic fragments [A or B indicates the correspondence of the fragment with tryptic fragments A or B (Figure 1)]; th indicates the bands that correspond to thermolysin.

samples (1 mg/mL SR vesicles, 50 mM MES, pH 6.0, 100 mM KCl, and 20% glycerol) by dialysis against Chelex 100, at 4 °C overnight. An aliquot was then withdrawn and incubated with 200 μM [^{14}C]DCCD for 2 h as described above.

The stoichiometry of DCCD binding was determined by measuring the amount of radioactive tracer. For this purpose, SR vesicles (1 mg in 1 mL) were labeled with [^{14}C]DCCD as described above. Following the 2-h incubation, the reaction was stopped by precipitating the protein with 5% trichloroacetic acid (final concentration) and delipidated as described by Martonosi (1976). The last pellet was air-dried and solubilized in 1% SDS. Aliquots were then withdrawn for protein and radioactivity determinations.

Electrophoresis. Polyacrylamide slab gel electrophoresis was performed by the methods of Weber and Osborn (1969) on 7.5% polyacrylamide gels (run at a constant current of 45 mA per gel for 16 h at 20 °C) and of Laemmli (1970) on 7–17% polyacrylamide gradient gels (run at a constant power of 10 W per slab for 4–5 h at 15 °C). Electrophoresis at pH 6.3 was carried out as described by Weber and Osborn (1969) but with a modified buffer (pH 6.3) containing 70 mM NaH_2PO_4, 30 mM Na_2HPO_4, and 0.1% SDS (run at a constant current of 130 mA per slab for 4–5 h). The denaturing buffer used to solubilize protein precipitated with trichloroacetic acid contained 2.5% lithium dodecyl sulfate (LDS) instead of SDS to avoid precipitation at very acidic pH. Gels were loaded with 20–50 μg of protein per well and were stained by the Fairbanks method (Fairbanks, 1971). The molecular weight standards were β-galactosidase (116 000), phosphorylase *b* (97 000), bovine serum albumin (66 000), ovalbumin (45 000), glyceraldehyde-3-phosphate dehydrogenase (36 000), carbonic anhydrase (29 000), trypsinogen (24 000), trypsin inhibitor (20 100), and α-lactalbumin (14 200).

FITC Detection in the Gels. The fluorescence of electrophoretic bands labeled with FITC was photographed before staining by using a UV light box (excitation wavelength 310 nm) and placing a Corning 3-70 cutoff filter in front of the camera lens (Polaroid MP-4 land camera).

Autoradiography. Gels were processed for detection of ^{32}P radioactivity as follows: the stained gels were first photographed and then dried in a Bio-Rad slab gel dryer, Model 443. Radioactivity detection was then obtained by using Kodak X-OMAT X-ray film and a Cronex Quanta III intensifying screen. Autoradiography was carried out at −70 °C.

^{14}C radioactivity was detected as follows: the stained gels were photographed and then processed according to Bonner and Laskey (1974) or soaked in Amplify (Amersham) for fluorographic detection of the radioactivity. Then they were dried and processed for autoradiography as above.

ATPase Activity. Calcium-dependent ATPase activity was followed by the colorimetric determination of P_i described by Lanzetta et al. (1979), using the following conditions: 0.01 mg of SR protein/mL, 20 mM MOPS, pH 7.0, 80 mM KCl, 5 mM $MgCl_2$, 0.1 mM $CaCl_2$, 0.1 mM EGTA, 3 μM A23187, and 1 mM ATP.

Calcium Binding. This was determined by equilibration of the SR ATPase with ^{45}Ca in chromatography columns as described by Inesi et al. (1980), with a medium containing 20 mM MOPS, pH 7.0, 80 mM KCl, 5 mM $MgCl_2$, 60 μM $CaCl_2$, and 50 μM EGTA. These conditions yield saturation of the high-affinity sites which are involved in ATPase activation of calcium transport.

Phosphoenzyme Levels. Phosphorylation of SR ATPase with ATP was carried out in a mixture containing 0.5 mg of protein/mL in the presence of 20 mM MOPS, pH 7.0, 80 mM KCl, 5 mM $MgCl_2$, 0.1 mM $CaCl_2$, 0.1 mM EGTA, and 1 mM [γ-^{32}P]ATP. Following incubation for 30 s at 4 °C, the reaction was stopped with 5% trichloroacetic acid and 4 mM P_i (final concentration). Phosphorylation with P_i was performed with 0.5 mg/mL SR protein in 20 mM MES–Tris, pH 6.0, 5 mM $MgCl_2$, 1 mM EGTA, and 5 mM [^{3i}P]P_i for 5 min at 25 C and stopped with 0.25 M perchloric acid and 4 mM P_i (final concentration). In both cases, the samples were washed 5 times by centrifugations and suspensions with a solution containing 0.125 M perchloric acid and 2 mM P_i. The

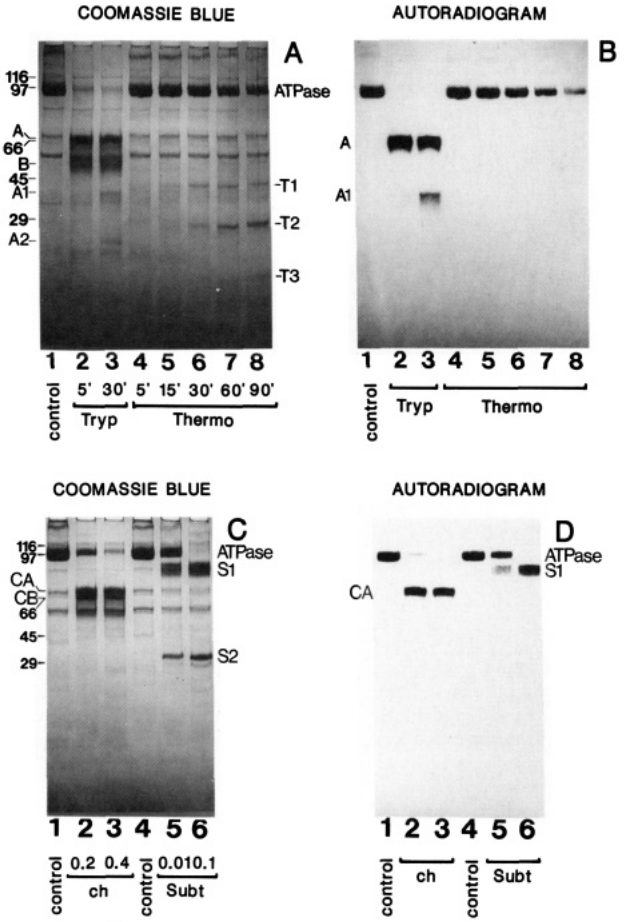

FIGURE 3: ^{32}P labeling pattern of proteolytic ATPase fragments following incubation of predigested SR vesicles with [γ-^{32}P]ATP and Ca^{2+}. Electrophoretic patterns were obtained by electrophoresis at acidic pH (see Materials and Methods). Peptide bands were stained with Coomassie blue (panels A and C), and the ^{32}P label was evidenced by autoradiography (panels B and D). Undigested SR vesicles are shown in column 1 (panels A and B) and in columns 1 and 4 (panels C and D). Samples digested with trypsin (0.005 trypsin/SR ratio) for 5 or 30 min are shown in columns 2 and 3 (panels A and B), respectively. Samples digested with thermolysin (0.5 thermolysin/SR ratio) for 5, 15, 30, 60, or 90 min are shown in columns 4, 5, 6, 7, and 8 (panels A and B), respectively. Samples digested with chymotrypsin for 60 min (panels C and D) at a 0.2 or 0.4 chymotrypsin/SR ratio are shown in columns 2 and 3. Samples digested with subtilisin for 30 min (panels C and D) at a 0.01 or 0.1 subtilisin/SR ratio are shown in columns 5 and 6. A, B, A_1, and A_2 and T_1, T_2, and T_3 indicate ATPase tryptic and thermolytic fragments (panels A and B). CA and CB and S_1 and S_2 indicate ATPase chymotryptic fragments and ATPase fragments obtained with subtilisin (panels C and D).

final pellets were dissolved in 0.1 N NaOH, 2% Na_2CO_3, 2% SDS, and 5 mM NaH_2PO_4, and processed for determinations of protein and ^{32}P radioactivity.

RESULTS

Patterns of Proteolytic Digestion. Our first objective was to compare the electrophoretic patterns of SR ATPase proteolytic digestion, using four different proteases: trypsin (whose pattern is already known (Thorley-Lawson & Green, 1973; MacLennan et al., 1985), α-chymotrypsin, thermolysin, and subtilisin.

Trypsin. The initial trypsin cleavage of SR ATPase occurs at Arg-505 (MacLennan et al., 1985; Brandl et al., 1986), producing the two fragments A and B, with subsequent cleavage of A at Arg-198 (MacLennan et al., 1985; Brandl et al., 1986) producing fragments A_1 and A_2. It is shown in

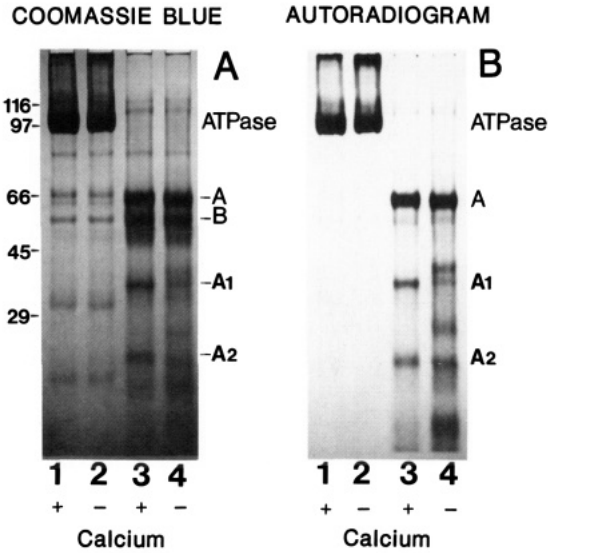

FIGURE 4: DCCD labeling pattern of SR ATPase digested with trypsin. SR vesicles were first incubated with DCCD at a high DCCD/SR ratio (see Materials and Methods), in the presence (columns 1 and 3) and in the absence (columns 2 and 4) of 50 μM Ca^{2+}. SR vesicles (columns 1 and 2) were then digested with trypsin (0.005 trypsin/SR ratio) for 30 min, and the samples were subjected to electrophoresis (columns 3 and 4) according to Weber and Osborn (1969). Panel A shows Coomassie blue staining of the gel, and panel B shows the corresponding autoradiogram.

Figure 1C (lane 2) that although the Laemmli (1970) electrophoretic procedure yields very sharp bands, the A and B fragments are not resolved. On the other hand, good resolution (lanes 2 and 3 in Figure 1A) of the A and B fragments, as well as the A_1 and A_2 fragments, is obtained by the Weber and Osborn (1969) procedure. While the theoretical (based on the amino acid sequence) molecular weights of the A, B, A_1, and A_2 fragments are 55 394, 54 973, 33 279, and 22 115 (Brandl et al., 1986), respectively, the observed molecular weight values (lanes 2 and 3 in Figure 1A) are approximately 65 000, 55 000, 35 000, and 20 000, respectively.

Chymotrypsin. The initial cleavage of SR ATPase by chymotrypsin yields the two fragments CA and CB, which migrate with molecular weights of 52 000 and 62 000 in the Laemmli system (lanes 3 and 4 in Figure 1C) and 64 000 and 60 000 in the Weber and Osborn system (lanes 5 and 6 in Figure 1A). The similar size of the first two tryptic and chymotryptic fragments and the labeling pattern (see below) suggest that the two enzymes cleave at the same domain in the ATPase structure.

It is apparent from Figure 1 that fragment CB does not accumulate in proportion to fragment CA. Therefore, fragment CB undergoes digestion at a faster rate than CA. Several subfragments produced by prolonged digestion with chymotrypsin are noted in Figure 1. On the basis of the distribution of labels (see below), the origin of some subfragments can be attributed to CA or CB. It is noteworthy that if the preparation is centrifuged following digestion with chymotrypsin, and samples of sediment and supernatant are subjected to electrophoretic analysis, subfragments CB_1 and CB_2 are found in the supernatant fraction. In fact, these two subfragments are released into the medium following their cleavage, and, for this reason, we assume that they are soluble in aqueous media. This may turn out to be a convenient feature for peptide separation on a preparative scale.

Thermolysin. It is shown in Figure 2A that digestion of SR ATPase with thermolysin produces fragments of a wide range of sizes, with no accumulation of large size fragments

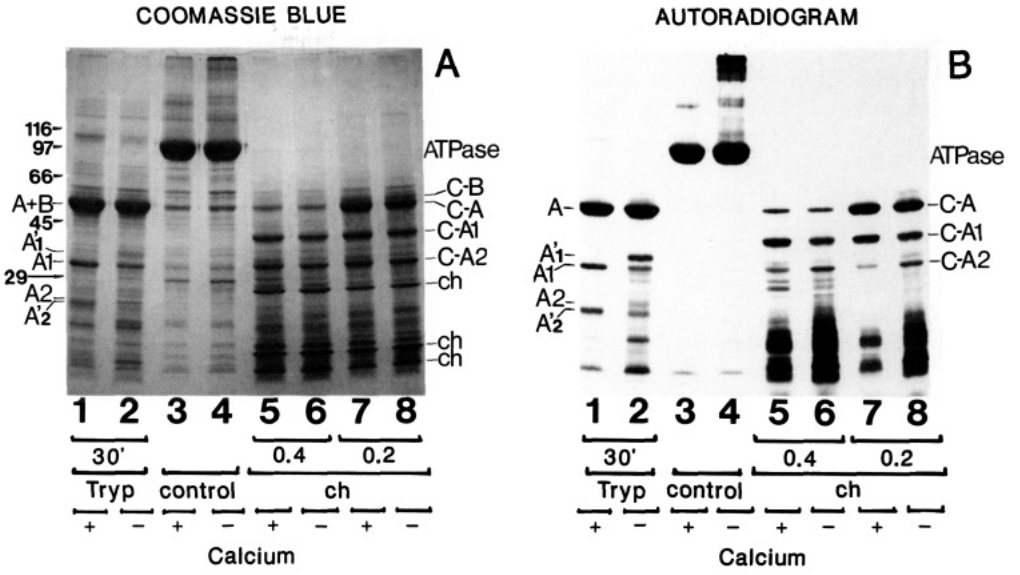

FIGURE 5: DCCD labeling pattern of SR ATPase digested with trypsin or chymotrypsin. SR vesicles were incubated with DCCD at a high DCCD/SR ratio (see Materials and Methods), in the presence (columns 1, 3, 5, and 7) and in the absence (columns 2, 4, 6, and 8) of 50 μM Ca^{2+}. SR vesicles (columns 3 and 4) were then digested with trypsin (0.005 trypsin/SR ratio) for 30 min (columns 1 and 2) or with chymotrypsin at a 0.2 (columns 7 and 8) or 0.4 (columns 5 and 6) chymotrypsin/SR ratio for 60 min. Samples were then subjected to electrophoresis according to Laemmli (1970). Panel A shows Coomassie blue staining of the gel, and panel B shows the corresponding autoradiogram. A+B, A'_1, A_1, A_2, and A'_2 correspond to SR ATPase tryptic fragments; CA, CB, CA_1, CA_2, CB_1, and CB_2 correspond to SR ATPase chymotryptic fragments; ch indicates chymotrypsin subunits visible in the gel. Note that the presence of radioactive DCCD labeling in bands migrating with molecular weights analogous to the chymotrypsin subunits is in fact due to overlapping ATPase fragments, since chymotrypsin was never exposed to free DCCD in these experiments.

as observed with trypsin or chymotrypsin (Figure 1). This suggests that thermolysin acts simultaneously on different segments of the ATPase chain (even though it may actually bind to a single domain of the ATPase three-dimensional structure). Some of the resulting peptides (T_1–T_9 in Figure 2A) can be compared with the large tryptic fragments (A and B) on the basis of their labeling patterns (see below). In fact, T_8 is labeled with FITC in analogy to tryptic fragment B. Furthermore, T_2 and T_3 are not labeled with DCCD, also in analogy to fragment B. On the other hand, T_{4-7} and T_9 are labeled with DCCD in analogy to fragment A.

Subtilisin. It is shown in Figure 1C (lanes 6 and 7) that subtilisin, due to its low selectivity with respect to peptide substrates, cleaves the SR ATPase into a large number of fragments. This may be advantageous for recovery of labels in small fragments.

FITC Labeling. Incubation of SR ATPase with FITC results in covalent labeling of the Lys-515 residue (Brandl et al., 1986) and loss of the enzyme's ability to bind and utilize ATP as a substrate (Mitchinson et al., 1982; Andersen et al., 1982). In this case, as well as for the DCCD label (see below), it is possible to digest the protein after the labeling reaction. We observe that the FITC label is associated with the B fragment (lanes 2 and 3 in Figure 1A,B) when the labeled ATPase is digested with trypsin and subjected to electrophoretic analysis. The FITC is an aid for the assignment of small fragments derived from digestion with other proteolytic enzymes to tryptic fragment B (Figure 1).

It is of interest that no FITC label is detected in the larger fragments derived from ATPase digestion with thermolysin (Figure 2). The label appears instead in very small fragments (T_8) near or after the dye front. These observations suggest that the FITC-labeled Lys-515 is in a protein domain permitting rapid cleavage of very small labeled peptides by thermolysin.

This feature may be useful in preparative recovery of small, FITC-labeled peptides. The presence of known labeled residues in unknown peptides is an aid for the establishment of their identity.

Table I: DCCD Incorporation in the SR ATPase in the Presence and in the Absence of Exogenous Nucleophiles[a]

	calcium	nmol of DCCD/mg of protein
DCCD	+	2.5
DCCD	–	4.2
DCCD + GEE	+	1.6
DCCD + GEE	–	2.3
DCCD + EDA	+	1.4
DCCD + EDA	–	2.4

[a] SR vesicles (1 mg/mL) were labeled with 200 μM DCCD (see Materials and Methods) in the presence or in the absence of 50 μM $CaCl_2$ and either in the presence or in the absence of 0.2 M GEE or 0.1 M EDA.

Phosphoenzyme Formation and ^{32}P Labeling. Utilization of ATP by SR ATPase in the presence of Ca^{2+} includes formation of a phosphorylated enzyme intermediate (Yamamoto & Tonomura, 1967) by transfer of the ATP-terminal phosphate onto the Asp-351 (MacLennan et al., 1985; Brandl et al., 1986) residue of the ATPase protein. The enzyme retains its ability to form the phosphorylated intermediate even after being subjected to partial digestion with trypsin, since the large tryptic fragments remain joined by multiple weak interactions and do not separate unless completely solubilized with detergents (Rizzolo et al., 1976). For comparison, we have studied the ability of the SR ATPase to form the phosphoenzyme intermediate following digestion with several proteolytic enzymes and the distribution of ^{32}P label among the resulting proteolytic fragments. It should be pointed out that acid denaturation of the ATPase is required soon after the phosphoryl transfer reaction in order to stabilize the newly formed phosphoryl bond. Therefore, the proteolytic digestion must be carried out *before* the phosphoryl transfer reaction. Thus, the presence of ^{32}P label in the electrophoretic bands

reflects the distribution of the label among the proteolytic fragments *as well as* the extent of phosphoryl transfer activity retained by the ATPase following proteolytic digestion.

In agreement with previous observations (Thorley-Lawson & Green, 1973; Stewart et al., 1976), we found that the ^{32}P label is associated with tryptic fragment A and subfragment A_1 and not with fragment B or subfragment A_2 (lanes 2 and 3 in Figure 3B). On the other hand, following digestion with chymotrypsin, the ^{32}P label is only present in the CA fragment, and no label is found in any of the subfragments (lanes 2 and 3 in Figure 3D). This indicates that none of the chymotrypsin subfragments can be considered to be analogous to the A_1 trypsin subfragment with respect to the ability to acquire and/or retain the ATP-terminal phosphate.

It is also shown in Figure 3 (lanes 5 and 6 in panels C and D) that the ^{32}P label is only found in the first and largest ATPase fragment produced by light digestion with subtilisin. However, no ^{32}P label is found in any of the fragments produced by digestion with thermolysin (lanes 4–8 in Figure 3B), while the nondigested ATPase molecules retain their ability to acquire the label. This indicates that the ATPase undergoes multiple and simultaneous cuts as a consequence of light digestion with thermolysin, thereby undergoing denaturation and losing its ability to form the phosphorylated intermediate.

DCCD Labeling. Derivatization of SR with DCCD produces inhibition of calcium binding and ATPase activity when labeling is carried out in the absence of calcium (Pick & Racker, 1979; Murphy, 1981; Scofano et al., 1985). A preliminary characterization of DCCD labeling at high [^{14}C]-DCCD/protein ratios (i.e., maximal labeling) is shown in Figure 4. Electrophoresis by the Weber and Osborn (1969) procedure shows that the [^{14}C]DCCD label is associated with the tryptic fragment A and its subfragments, and not with fragment B. It is apparent that the patterns of labeling and the tryptic digestion of samples reacted with [^{14}C]DCCD in the presence or in the absence of Ca^{2+} are different.

Although the large tryptic fragments A and B are not separated by the Laemmli procedure, Figure 5 (lanes 1 and 2) shows again that the pattern of trypsin subfragmentation is different in samples incubated with DCCD in the presence as opposed to the absence of Ca^{2+}. A very interesting difference is related to the heavily labeled subfragment A'_1, which is present in the samples incubated with DCCD in the absence of Ca^{2+}. A change in the mobility of fragment A_2 when labeled (indicated in the autoradiogram as A'_2 in Figure 5) is noted. It is also apparent that labeling in the absence of Ca^{2+} produces cross-linking of entire enzyme chains, yielding large and heavily labeled bands on top of the gels.

While the tryptic fragments A and B are not separated by the Laemmli (1970) procedure, the corresponding chymotryptic fragments CA and CB are resolved satisfactorily. It can be shown then that the DCCD label is associated with the chymotryptic fragment CA (and subfragments) and not with fragment CB (Figure 5). It is also apparent that the labeling patterns in the presence and absence of Ca^{2+} are different. Calcium also affected labeling patterns in experiments on proteolytic digestion with subtilisin and thermolysin (not shown).

Since the samples incubated with DCCD in the absence of Ca^{2+} contained a fairly high concentration of EGTA, we checked whether the cross-linking observed under these conditions was, at least in part, due to DCCD-activated EGTA. In principle, the EGTA carboxyl groups could bind DCCD, forming a homobifunctional acylisourea that could react with amino groups on the protein. In a series of experiments in which we removed Ca^{2+} by prolonged dialysis against Chelex 100 (see Materials and Methods), we obtained essentially the same cross-linking and labeling pattern observed in the presence of EGTA. Therefore, EGTA did not contribute significantly to the labeling.

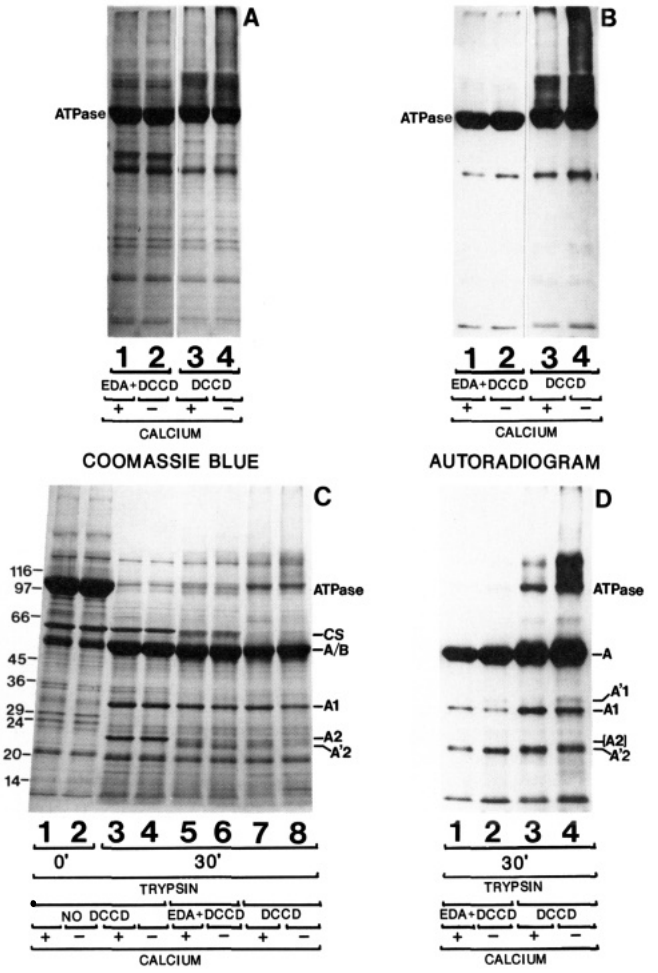

FIGURE 6: Patterns of radioactive DCCD labeling (high DCCD/SR ratio) in tryptic digests of the SR ATPase labeled with [^{14}C]DCCD in the presence and in the absence of EDA. SR vesicles (1 mg/mL) were labeled with 200 μM [^{14}C]DCCD (see Materials and Methods) either in the absence (panels A and B, columns 3 and 4; panels C and D, columns 7 and 8 and 3 and 4) or in the presence of 0.1 M EDA (panels A and B, columns 1 and 2; panels C and D, columns 5 and 6 and 1 and 2) are both in the presence (panels A and B, columns 1 and 3; panels C and D, columns 5 and 7 and 1 and 3) and in the absence (panels A and B, columns 2 and 4; panels C and D, columns 6 and 8 and 2 and 4) of 50 μM $CaCl_2$. Columns 1–4 in panel C correspond to the control, where the SR vesicles were processed like the other samples but in the absence of DCCD; also in the presence (columns 1 and 3) and in the absence (columns 2 and 4) of calcium. Notice that columns 1–4 in panel C are not present in panel D, since they were not exposed to DCCD. The SR vesicles were digested with trypsin (0.005 trypsin/SR ratio) (see Materials and Methods) for 30 min (panels C and D, columns 3–8 and 1–4). A/B corresponds to tryptic fragments A and B (panel C) and A to tryptic fragment A in the autoradiogram (panel D), since fragment B is not labeled by DCCD; A_1, A_2, A'_1, and A'_2 correspond to tryptic fragments derived form fragment A; [A_2] indicates the position of fragment A_2, shown in Coomassie blue stain (panel C, columns 3 and 4) as a reference in the autoradiogram; CS indicates calsequestrin in panel C. The electrophoresis was performed according to Laemmli (1970). Panels A and C show Coomassie blue stain, and panels B and D show the autoradiogram of the gel.

Labeling with High DCCD/SR Ratios in the Presence of Exogenous Nucleophiles. The experiments described above show that incubation of SR vesicles with DCCD produces multiple effects, including changes in electrophoretic mobility of proteolytic fragments and slower mobility of the main

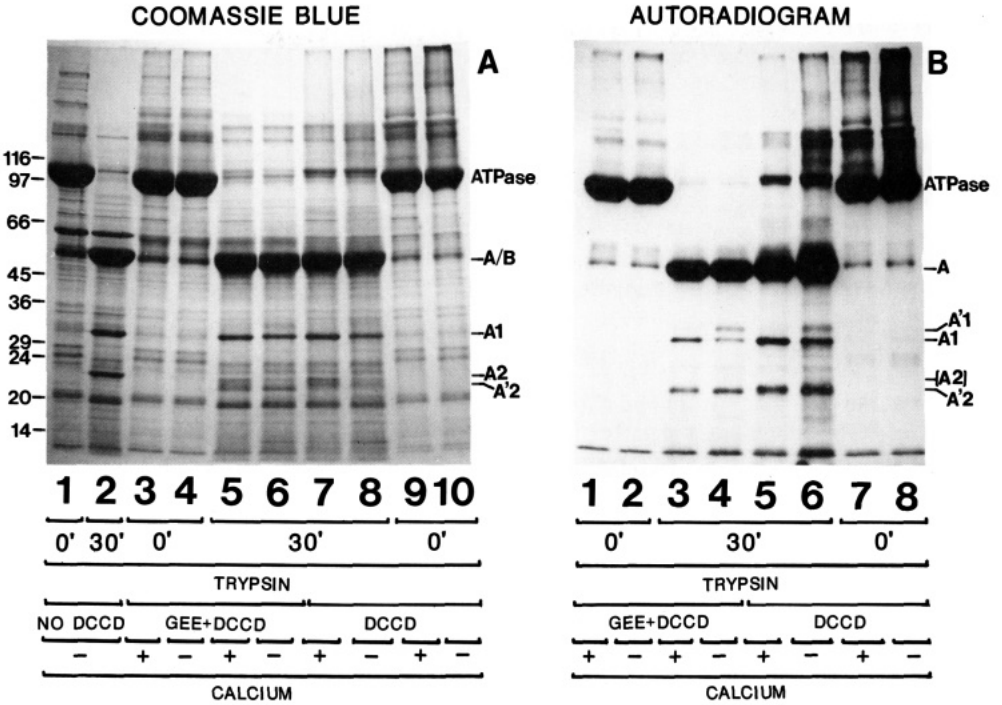

FIGURE 7: Patterns of radioactive DCCD labeling (high DCCD/SR ratio) in tryptic digests of the SR ATPase labeled with [^{14}C]DCCD in the presence or in the absence of GEE. SR vesicles (1 mg/mL) were labeled with 200 μM [^{14}C]DCCD (see Materials and Methods) either in the absence (panel A, columns 7–10; panel B, columns 5–8) or in the presence of 0.2 M GEE (panel A, columns 3–6; panel B, columns 1–4) and both in the presence (panel A, columns 3, 5, 7, and 9; panel B, columns 1, 3, 5, and 7) and in the absence (panel A, columns 4, 6, 8, and 10; panel B, columns 2, 4, 6, and 8) of 50 μM $CaCl_2$. Columns 1 and 2 of panel A correspond to the control, where the SR vesicles were processed as the other samples but in the absence of DCCD. Notice that columns 1 and 2 of panel A are not present in panel B since they were not exposed to DCCD. The SR vesicles were digested with trypsin (0.005 trypsin/SR ratio) (see Materials and Methods) for 30 min (panel A, columns 2 and 5–8; panel B, columns 3–6). A/B corresponds to tryptic fragments A and B (panel A) and A to tryptic fragment A in the autoradiogram (panel B), since fragment B is not labeled by DCCD; A_1, A_2, A'_1, and A'_2 correspond to tryptic fragments derived from fragment A; [A_2] indicates the position of fragment A_2, shown in Coomassie blue stain (panel A, column 2), as a reference in the autoradiogram (panel B). Electrophoresis was performed according to Laemmli (1970). Panel A shows Coomassie blue stain and panel B the autoradiogram of the gel.

ATPase band. These effects are due to intramolecular (i.e., within a single ATPase chain) and intermolecular (i.e., more than one ATPase chain) cross-linking between a carbodiimide-activated carboxylic acid and an endogenous nucleophile (Figure 10), interfering with the establishment of a relationship between derivatization of specific peptide fragments and inhibition of binding and catalytic reactions. It was reported, for instance, that the (Na,K)-ATPase is not inhibited by carbodiimide if internal cross-linking is prevented by the addition of exogenous nucleophiles (Pedemonte & Kaplan, 1986). Therefore, we have performed a series of SR ATPase derivatization experiments with [^{14}C]DCCD in the presence of exogenous nucleophiles.

It should be first pointed out that the stoichiometry of labeling is approximately twice as high in the absence as in the presence of Ca^{2+}. Addition of the exogenous nucleophiles ethylenediamine or glycine ethyl ester to the incubation medium reduces the stoichiometry of labeling approximately 50% in either case (Table I).

A very clear effect of the exogenous nucleophiles is to prevent intermolecular cross-linking of ATPase chains and the appearance of large radioactive bands on top of the gels [compare lanes 3B and 4B (and lanes 3D and 4D) with lanes 1B and 2B (and lanes 1D and 2D) in Figure 6; compare lanes 7B and 8B with lanes 1B and 2B in Figure 7]. Furthermore, calsequestrin is completely cross-linked and disappears from the gels following derivatization with DCCD (lanes 7 and 8 in Figure 6), an effect that is to some extent prevented by the presence of exogenous nucleophiles (lanes 5 and 6 in Figure 6).

The electrophoretic resolution of proteolytic fragments is sharper if exogenous nucleophiles are present during the incubation with DCCD (band A'_2 in lanes 5 and 6 as compared to lanes 7 and 8 in Figure 6). This may be due to prevention of intramolecular cross-linking.

A most important finding is that even in the presence of exogenous nucleophiles, calcium has a definite influence on the extent (Table I) and the pattern of labeling. It is clear that band A'_2 is more heavily labeled and the labeled A'_1 band is present only in samples derivatized in the absence of calcium (lanes 1 and 2 in Figure 6D and lanes 3 and 4 in Figure 7B).

As for the functional effects of incubaions with high DCCD/SR ratios, we confirm a strong inhibition on calcium binding (Pick & Racker, 1979; Scofano et al., 1985) and on other partial reactions (Scofano et al., 1985). This inhibitory effect is to a great extent prevented if calcium is present during the incubation with DCCD (Figure 9). It can be also shown that the exogenous nucleophiles afford some protection, but not nearly as much as calcium.

Labeling with Low DCCD/SR Ratios in the Presence of Exogenous Nucleophiles. Since the type of functional inactivation depends on the extent of ATPase derivatization with DCCD (Scofano et al., 1985), we characterized the distribution of label after derivatization with low DCCD/SR ratios in the presence of exogenous nucleophiles. In this case, recovery of a detectable autoradiographic signal required use of high specific activity in the label and a prolonged exposure of the films. In fact, the stoichiometry of radioactive labeling was extremely low, even though the resulting functional inhibition (see below) indicates that the majority of the ATPase chains

are affected by the derivatization procedure. Owing to the very prolonged exposure of the films, small protein contaminants (such as X and Y in lanes 1 and 2 of Figure 8B) appear radioactive in this type of experiment, while no radioactivity is detected when high DCCD/SR ratios are used (lanes 1 and 2 in Figure 7B). Therefore, it is difficult to evaluate the labeling of tryptic fragment A_1, owing to its electrophoretic overlap with band X (Figure 8).

A clear radioactive signal is obtained only in the absence of Ca^{2+}, in correspondence of band A'_2 (lane 4 in Figure 8B). However, the radioactive signal corresponds to an extremely low amount of protein, since a corresponding band is hardly evidenced by Coomassie Blue staining (lane 8 in Figure 8A), while the A_2 band is very clearly stained. It is apparent then that in this case the radioactive adduct has a slightly higher electrophoretic mobility. However, contrary to the experiments with high DCCD/SR ratios (Figures 6 and 7), most of the A_2 fragment is not labeled when SR is incubated with low DCCD/SR ratios.

As for the functional effects of incubations with low DCCD/SR ratios, we confirm that 30–35% inhibition of the $EP + H_2O \rightleftharpoons E + P_i$ reaction (panels C and D in Figure 9) is obtained in these conditions, while calcium binding and ATPase phosphorylation with ATP (panels A and B in Figure 9) are not inhibited. The observed inhibition is largely prevented when the incubation is carried out in the presence of calcium. Exogenous nucleophiles do not have a significant effect in this case (panel D in Figure 9).

Discussion

Proteolytic and Labeling Patterns. Our comparative experiments on proteolytic cleavage of SR ATPase show that trypsin and chymotrypsin yield large fragments of similar size. Considering the different specificity of the two enzymes for peptide-bond substrates, these observations suggest that trypsin and chymotrypsin bind to the same ATPase domain. Thereby, cleavage sites for these two enzymes may be located within a small distance, and peptide fragments of similar size (A ≃ CA; B ≃ CB) are produced. A similar explanation was given for the similar fragments produced by proteolytic cleavage of heavy meromyosin with trypsin and papain (Tonomura & Oosawa, 1972) or of immunoglobulins with papain and pepsin (Edelman & Gall, 1969). Digestion of the SR ATPase with chymotrypsin in different conditions produces a slightly different pattern (Andersen & Jorgensen, 1985).

No large fragments of size similar to tryptic fragments A and B were observed following digestion of SR ATPase with thermolysin and subtilisin, probably due to simultaneous cleavage of several peptide bonds, which yields the different patterns obtained with these enzymes.

The association of the ^{32}P label with the A and A_1 tryptic fragments, and of the FITC label with the B tryptic fragment (Figure 11), has been already established (Thorley-Lawson & Green, 1973; Stewart et al., 1976; Mitchinson et al., 1982). This information is helpful in the comparative assignment of fragments obtained by digestion with other enzymes. The analogy of the chymotryptic fragment CA to the tryptic fragment A is demonstrated by the incorporation of the ^{32}P label. Further fragmentation of the ATPase by chymotrypsin, thermolysin, or subtilisin, however, produces denaturation of the ATPase, thereby preventing ATP utilization and incorporation of the ^{32}P label, and therefore further identification of these fragments with ^{32}P was not possible.

The analogy of the tryptic fragments B and the chymotryptic fragment CB is established by the presence of FITC

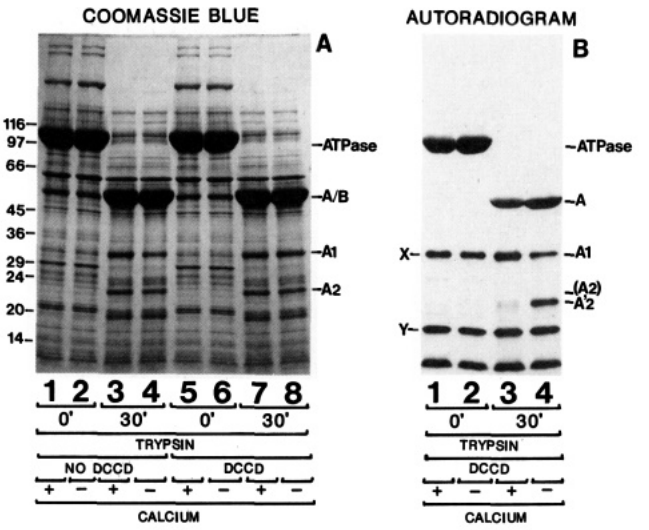

FIGURE 8: Patterns of radioactive DCCD (low DCCD/SR ratio) in tryptic digests of the SR ATPase labeled with [^{14}C]DCCD in the presence and in the absence of calcium. SR vesicles (1 mg/mL) were incubated with 10 μM [^{14}C]DCCD (see Materials and Methods) in the presence (panel A, columns 5 and 7; panel B, columns 1 and 3) and in the absence (panel A, columns 6 and 8; panel B, columns 2 and 4) of 50 μM $CaCl_2$. Columns 1–4 in panel A correspond to the control, where the SR vesicles were processed as the other samples but in the absence of DCCD. Notice that columns 1–4 of panel A are not present in panel B since they were not expossed to DCCD. The SR vesicles were digested with trypsin (0.005 trypsin/SR ratio) for 30 min (panel A, columns 3, 4, 7, and 8; panel B, columns 3 and 4). A/B corresponds to tryptic fragments A and B (panel A) and A to tryptic fragment A in the autoradiogram (panel B), since fragment B is not labeled by DCCD; A_1, A_2, and A'_2 correspond to tryptic fragments derived from fragment A; [A_2] indicates the position of fragment A_2, shown in Coomassie blue stain (panel A), as a reference in the autoradiogram. Electrophoresis was carried out according to Laemmli (1970). Panel A shows Coomassie blue stain and panel B the autoradiogram of the gel.

in both fragments. The latter is larger, indicating that the cleavage site of chymotrypsin is closer to the amino terminus than the tryptic site. The FITC labeling of CB_1, CB_2, and smaller fragments obtained with chymotrypsin, thermolysin, and subtilisin is particularly useful, since several of these fragments are released into the medium and can be separated from the membrane-bound protein simply by centrifugation.

DCCD Labeling Patterns. A promising approach to the establishment of structure–function relationships is DCCD labeling, owing to the functional inactivation produced by this label. However, the occurrence of inter- and intramolecular cross-linking on the ATPase reacted with DCCD (Figures 6 and 7), the inhibition of specific ATPase partial reactions in the absence of calcium, and the effects of exogenous nucleophiles demonstrate the complexity of the DCCD reactions with the ATPase protein. The possible pathways for transformation of the initial [^{14}C]DCCD adduct with a carboxyl residue in the ATPase are outlined in Figure 10. Formation of the initial *O*-acylisourea (**1** in Figure 10) and its rearrangement (**3** in Figure 10) are reactions producing radioactive labeling and possible inactivation of catalytic function. On the other hand, cross-linking with an endogenous nucleophile (**4** in Figure 10) or substitution by an exogenous nucleophile (**5** in Figure 10) may also provide inactivation of catalytic function without retention of the radioactive label.

In our experiments, we find clear evidence of extensive cross-linking of DCCD-reacted ATPase, as revealed by anomalous electrophoretic separation of both the ATPase and its proteolytic fragments (Figures 6 and 7). Intermolecular cross-linking (possibly facilitated by an aggregated state of

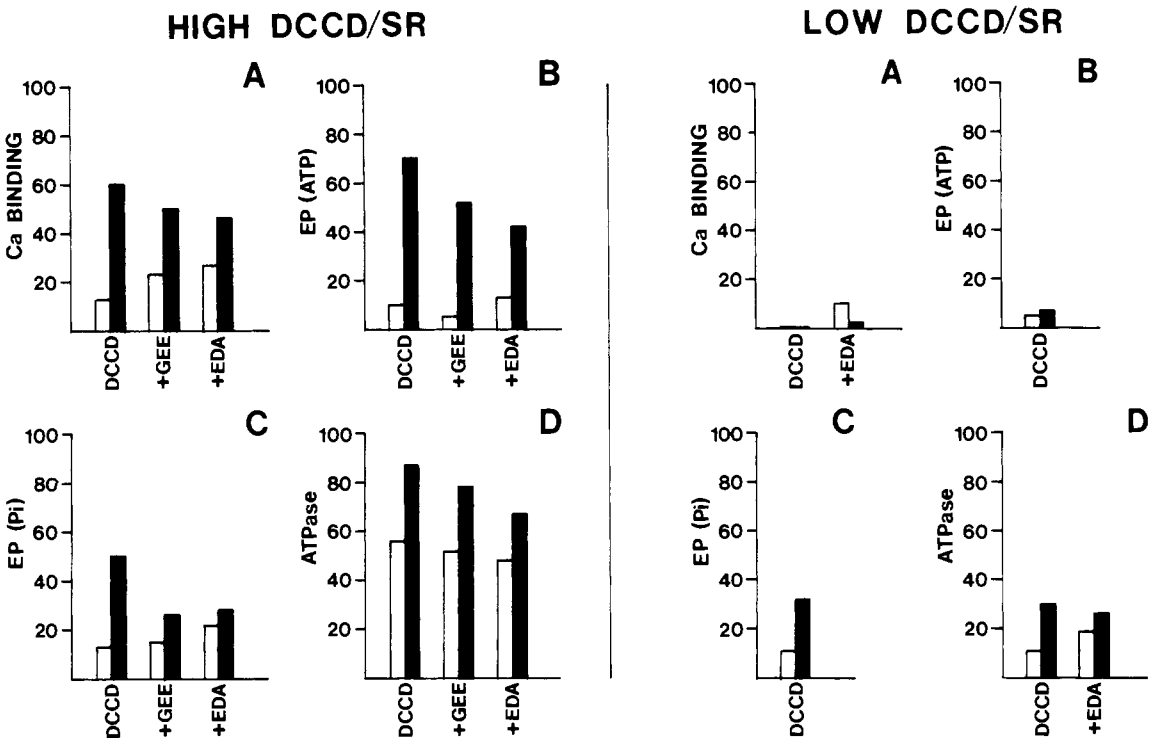

FIGURE 9: Inhibition of calcium binding, EP formation by ATP and P_i, and ATPase activity of the SR ATPase by DCCD at high and at low DCCD/SR ratios. SR vesicles (1 mg/mL) were incubated with 200 μM (high DCCD/SR ratio) or 10 μM (low DCCD/SR ratio) DCCD and the carbodiimide plus either 0.2 M GEE or 0.1 M EDA, both in the presence (white bars) and in the absence (black bars) of 50 μM $CaCl_2$, as described under Materials and Methods. Calcium binding (A) (control levels, 7.7 ± 0.4 nmol/mg), EP formation by ATP (B) (control levels, 3.5 ± 0.3 nmol/mg), EP formation by P_i (C) (control levels, 3.3 ± 0.4 nmol/mg), and ATPase activity (D) (control levels, 3.1 ± 0.3 μmol mg^{-1} min^{-1}) measurements were carried out as described under Materials and Methods. The results are shown as the percentage of enzyme inhibition.

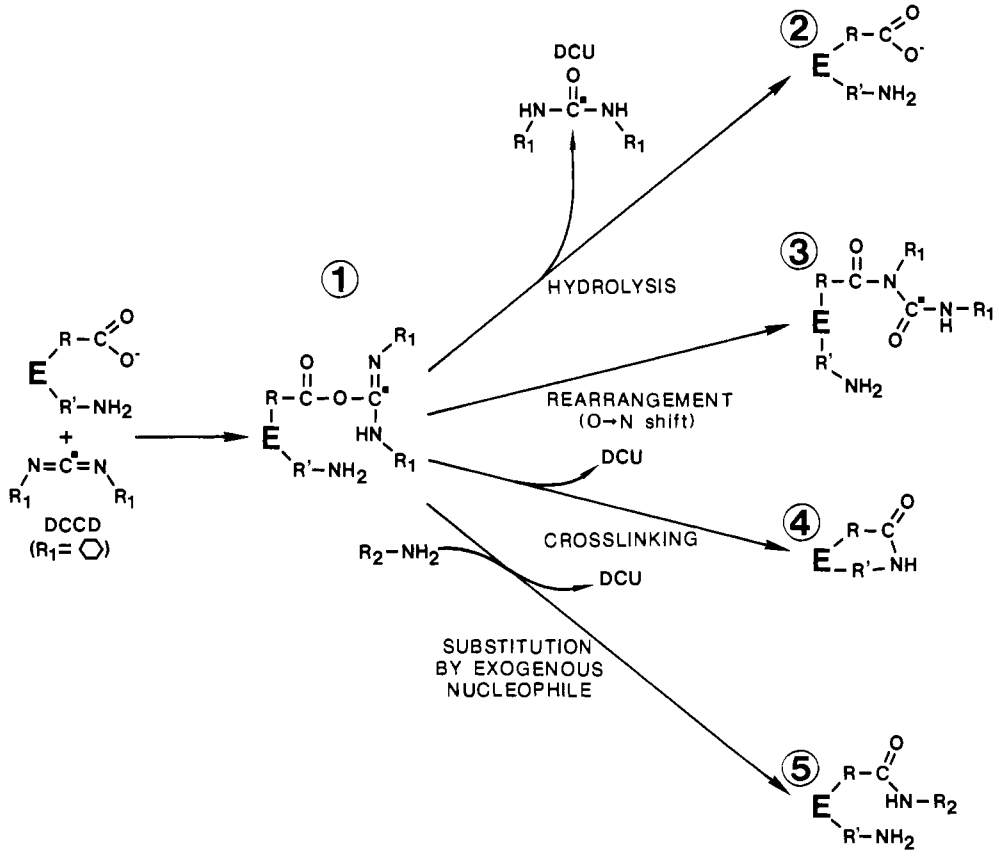

FIGURE 10: Reaction of a carboxyl group of an enzyme (E) with DCCD and secondary reaction pathways of the *O*-acylisourea. **1** corresponds to the labile *O*-acylisourea adduct formed by the reaction of DCCD (radioactively labeled at the C*) with a carboxyl group. The *O*-acylisourea can then undergo various reactions: (a) hydrolysis, producing the native enzyme (**2**) and dicyclohexylurea (DCU), with subsequent loss of the radioactive label by the enzyme; (b) rearrangement by an O → N acyl shift, producing a stable *N*-acylisourea (**3**), radioactive labeling of the enzyme, and block of residue R; (c) cross-linking (**4**) produced by nucleophilic attack of a nearby enzyme residue (R′), which yields DCU, loss of the label by the enzyme, and block of residues R and/or R′; (d) reaction with an exogenous nucleophile (R_2–NH_2) (**5**) (if present during the reaction with DCCD), which produces loss of DCU with the label and blocks residue R, but avoids internal cross-linking (Williams & Ibrahim, 1981).

the enzyme when no calcium is present) is completely prevented by addition of exogenous nucleophiles, that only partially prevents the cross-linking within the same chain. We find, however, that specific inactivation of the hydrolytic (EP + $H_2O \rightleftharpoons E + P_i$) ATPase reaction is produced by incubations with low DCCD/SR ratios, without significant incorporation of radioactive label, even in the presence of exogenous nucleophiles. This suggests that blockage of catalytically active residues is produced by internal cross-linking in a location that is not readily accessible to exogenous nucleophiles. Alternatively, it is possible that the exogenous nucleophile blocks the catalytically active residue (**5** in Figure 10). Neither of these reactions allows retention of radioactive label (Figure 10).

Incubation with high DCCD/SR ratios yield significant incorporation of radioactive label (Table I) even in the presence of exogenous nucleophiles. It is clear that tryptic fragment B (as well as the chymotryptic fragment CB; Figure 5) is not labeled at all (Figure 4). Labeling of fragment A and its subfragments is best observed when cross-linking and anomalous electrophoretic behavior are prevented by exposing the samples to exogenous nucleophiles (lanes 1 and 2 in Figure 6D and lanes 3 and 4 in Figure 7B). Under these conditions, tryptic fragment A_2 is labeled, and the extent of labeling is reduced when the DCCD incubation is carried out in the presence of calcium. An analogous protection by calcium is observed with respect to the stoichiometry of labeling (Table I) and to functional inactivation (Figure 9). Therefore, it is apparent that labeling of residues in fragment A_2 is causally related to functional inactivation. The inactivation produced by labeling of these residues must be specifically related to calcium binding, since inactivation of the hydrolytic reaction alone can be produced by DCCD without significant incorporation of radioactive label. It is known that subfragment A_2 contains several negatively charged residues which are likely to participate in calcium complexation (MacLennan et al., 1985) and to react with DCCD.

In addition to fragment A_2, tryptic fragment A_1 is also labeled. In this case, labeling is not reduced by the presence of calcium. It is of interest that the labeled fragment A_1 is split in two bands when the DCCD incubation is performed in the absence of calcium (lane 4 in Figure 7B). This splitting is not produced in the presence of calcium (lane 3 in Figure 7B), indicating that the presence of calcium prevents internal cross-linking in fragment A_1. Therefore, the conformation of fragment A_1 is sensitive to calcium binding.

In conclusion, our experiments on derivatization of the SR ATPase with [^{14}C]DCCD demonstrate that, under certain conditions, inactivation of ATPase hydrolytic activity is produced without significant incorporation of radioactive label. This type of inactivation is due to reaction following the initial formation of the [^{14}C]DCCD adduct and does not affect calcium binding.

Under different conditions of derivatization, inhibition of calcium binding and also radioactive labeling are observed. The distribution pattern of the label suggests that residues in fragment A_2, which are labeled only when the derivatization is carried out in the absence of calcium, are normally involved in calcium complexation and prevented from doing so by the presence of the label. On the other hand, the A_1 fragment is labeled both in the absence and in the presence of calcium, but it undergoes cross-linking (i.e., anomalous electrophoretic behavior) only when the derivatization is carried out in the absence of calcium. This indicates that in the absence of calcium, juxtaposition of nucleophilic residues with the initial DCCD adduct in the A_1 fragment is favored. It is likely that fragment A_1 participates (with A_2) in formation of the calcium binding domain, contributing residues other than those labeled with DCCD.

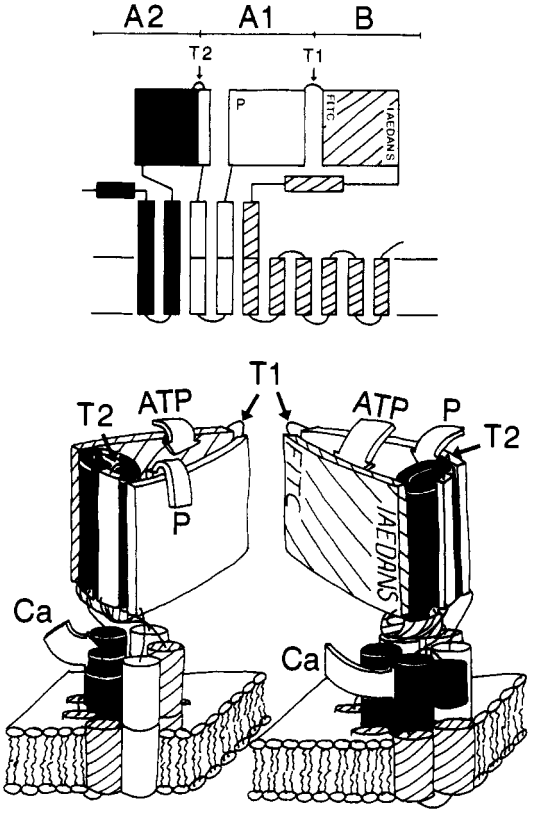

FIGURE 11: Diagram representing the relative positions of labels and active residues within the ATPase protein. A model based on the secondary structure given by MacLennan et al. (1985) is transformed into a folded configuration based on labeling patterns. The folded configuration (bottom) is given in two views, one rotated 90° from the other. The A_1, A_2, and B tryptic fragments are shade-coded in white, black, and dashed lines, respectively. P refers to the Asp-351 residue phosphorylated by ATP (planar model), FITC to the label on Lys-515, and IAEDANS to the label on Cys-670 and Cys-674. The cytoplasmic portion of the B fragment is folded over those of A_1 and A_2 fragments (in a trigonal arrangement), forming a cleft for ATP binding (Squier et al., 1987). The stalk regions and transmembrane helices are clustered to form a channel allowing calcium binding below the ATP binding and phosphorylation domains. The A_1 and A_2 fragments are in close proximity both within the cytoplasmic head and in the stalk region, contributing residues that participate in calcium binding.

Location of labels within the ATPase secondary structure is helpful in understanding the relationship of peptide segments and labeled residues within a folded conformation of the protein (Figure 11). We have previously determined by fluorescence spectroscopy (Squier et al., 1987) that IAEDANS labels placed on Cys-670 and Cys-674 (Bishop et al., 1987) of the B fragment are approximately 60 Å distant from the FITC label (Lys-515) and only 16–18 Å from a lanthanide occupying the calcium binding site. If, based on our present observations, we place the calcium binding domain in correspondence of the negatively charged residues in the A_2 fragment stalk region, we derive a configuration whereby the cytoplasmic portion of the B fragment (dashed lines in Figure 11) folds over those of the A_1 and the A_2 fragments, bringing into proximity the IAEDANS binding site and the calcium binding domain, assuming that the cytoplasmic portion of fragment A_2 is between A_1 and B in a trigonal arrangement. It can be also assumed that both the helices that form the stalk region and the transmembrane helices are clustered, again bringing into proximity the A_2 and A_1 segments which both contribute to formation of the calcium binding domain.

ACKNOWLEDGMENTS

We thank Thomas C. Squier, Diana J. Bigelow, and Mary E. Kirtley for many helpful discussions.

Registry No. ATPase, 9000-83-3; EDA, 107-15-3; GEE, 459-73-4; DCCD, 538-75-0; FITC, 27072-45-3; Ca, 7440-70-2; trypsin, 9002-07-7; chymotrypsin, 9004-07-3; thermolysin, 9073-78-3; subtilisin, 9014-01-1.

REFERENCES

Allen, G., & Green, N. M. (1976) *FEBS Lett. 63*, 188–192.
Andersen, J. P., & Jorgensen, P. L. (1985) *J. Membr. Biol. 88*, 187–198.
Andersen, J. P., Moller, J., & Jorgensen, P. L. (1982) *J. Biol. Chem. 257*, 8300–8307.
Andersen, J. P., Vilsen, B., Collins, J. H., & Jorgensen, P. L. (1986) *J. Membr. Biol. 93*, 85–92.
Baba, A., Nakamura, T., & Kawakita, M. (1986) *J. Biochem. (Tokyo) 100*, 1137–1147.
Bishop, J. E., Squier, T. C., Bigelow, D. J., & Inesi, G. (1987) *Proceedings of the First Symposium of the Protein Society*, San Diego, CA (Abstract 1109).
Bonner, W. M., & Laskey, R. A. (1974) *Eur. J. Biochem. 46*, 83–88.
Brandl, C. J., Green, N. M., Korczak, B., & MacLennan, D. H. (1986) *Cell (Cambridge, Mass.) 44*, 597–607.
Chadwick, C. C., & Thomas, E. W. (1983) *Biochim. Biophys. Acta 730*, 201–206.
Champeil, P., Buschlen, S., & Guillain, F. (1981) *Biochemistry 20*, 1520–1524.
Ebashi, S., & Lipman, F. (1962) *J. Cell Biol. 14*, 389–400.
Edelman, G., & Gall, W. (1969) *Annu. Rev. Biochem. 38*, 415–466.
Eletr, S., & Inesi, G. (1972) *Biochim. Biophys. Acta 282*, 174–179.
Fairbanks, G., Steck, T. L., & Wallach, D. F. (1971) *Biochemistry 10*, 2606–2617.
Hasselbach, W., & Makinose, M. (1961) *Biochem. Z. 333*, 518–528.
Hasselbach, W., & Makinose, M. (1963) *Biochem. Z. 339*, 95–111.
Inesi, G. (1985) *Annu. Rev. Physiol. 47*, 573–601.
Inesi, G., Kurzmack, M., Coan, C., & Lewis, D. (1980) *J. Biol. Chem. 255*, 3025–3031.
Laemmli, U. K. (1970) *Nature (London) 227*, 680–685.
Lanzetta, P. A., Alvarez, L. J., Reinsch, P. S., & Candia, O. A. (1979) *Anal. Biochem. 100*, 95–97.
Lowry, O. H., Rosebrough, N. J., Farr, A. L., & Randall, R. J. (1951) *J. Biol. Chem. 193*, 265–275.
MacLennan, D. H., Brandl, C. J., Korczak, B., & Green, N. M. (1985) *Nature (London) 316*, 696–700.
Martonosi, A. (1976) *FEBS Lett. 67*, 153–155.
Mitchinson, C., Wilderspin, A. F., Trinnaman, B. J., & Green, N. M. (1982) *FEBS Lett. 146*, 87–92.
Murphy, A. J. (1981) *J. Biol. Chem. 256*, 12046–12050.
Pedemonte, C., & Kaplan, J. (1986) *J. Biol. Chem. 261*, 3632–3639.
Pick, U., & Racker, E. (1979) *Biochemistry 18*, 108–113.
Rizzolo, L., LeMaire, M., Reynolds, J., & Tanford, C. (1976) *Biochemistry 15*, 3433–3437.
Saito, K., Immamura, Y., & Kawakita, M. (1984) *J. Biochem. (Tokyo) 95*, 1297–1304.
Saito-Nakatsuka, K., Yamashita, T., Kubota, I., & Kawakita, M. (1987) *J. Biochem. (Tokyo) 101*, 365–376.
Scofano, H. M., Barrabin, H., & Inesi, G. (1985) *Biochemistry 24*, 1025–1029.
Scott, T. L. (1986) *Biophys. J. 49*, 234a.
Squier, T. C., Bigelow, D. J., García de Ancos, J., & Inesi, G. (1987) *J. Biol. Chem. 262*, 4748–4754.
Stewart, P. S., MacLennan, D. H., & Shamoo, A. (1976) *J. Biol. Chem. 251*, 712–719.
Thorley-Lawson, D. A., & Green, N. M. (1973) *Eur. J. Biochem. 40*, 403–413.
Tonomura, Y., & Oosawa, F. (1972) *Annu. Rev. Biophys. Bioeng. 1*, 159–190.
Varga, S., Mullner, N., Pukula, S., Papp, S., Varga, K., & Martonosi, A. (1986) *J. Biol. Chem. 261*, 13943–13956.
Weber, K., & Osborn, M. (1969) *J. Biol. Chem. 244*, 4406–4412.
Williams, A., & Ibrahim, I. (1981) *Chem. Rev. 81*, 589–636.
Yamamoto, T., & Tonomura, Y. (1967) *J. Biochem. (Tokyo) 62*, 558–575.
Yamashita, T., & Kawakita, M. (1987) *J. Biochem. (Tokyo) 101*, 377–385.